CHARACTERISTICS ANALYSIS FOR HIGH-RISE BUILDINGS DURING TOP-DOWN CONSTRUCTION

Yuanhang WANG[1], Xiaoying PAN[2✉], Hui XU[1], Jinyang LIU[2],
Peizhen LI[2✉✉], Lingbo HE[1], Wenxin ZHANG[1]

[1] The First Construction Co., Ltd of China Construction Third Engineering Bureau Group, Wuhan, 430040, China
[2] State Key Laboratory of Disaster Reduction in Civil Engineering, Tongji University, Shanghai, 200092, China

Abstract. New advances in top-down construction are developing with the construction of supertall buildings in China. This study presents a finite element analysis for high-rise structural construction with a top-down method (TDM) considering complex environmental conditions. Based on this analysis model, the forces and the deformation of the diaphragm wall, beams, and soldier piles at various stages of construction are computed. Taking a super high-rise building with a 5-story basement in Nanjing as an example, the reliability and accuracy of the model is verified by comparing the measured and simulated results of displacement and stress values at various locations. The research results reveal the relationship between excavation depth, soil settlement and pile displacement, which is convenient for finding the optimal construction critical surface. It lays a foundation for the study of the critical height of the subsequent construction and facilitates the prediction of the weak link in the process. At present, this project is under construction, so this study has reference value for subsequent construction projects.

✉Corresponding author. E-mail: *2011517@tongji.edu.cn*
✉✉Corresponding author. E-mail: *lipeizh@tongji.edu.cn*

1. Introduction

With the rapid development of industrialization and urbanization, ground resources have been maximized, and high altitude and underground spaces have become the focus of today's architectural development. Ultrahigh and ultradeep buildings have emerged at this historic moment, accompanied by the derivation of new building technologies. The top-down method (TDM) is increasingly used in large deep foundation pit projects because of its unique technological principle and ability to adapt to complex building environments.

To shorten construction schedules, the concept of top-down construction was first proposed in Japan (Wang, 2011). The TDM needs to be optimized according to the needs of different projects. Therefore, much theoretical research on the TDM has been conducted.

The research method of TDM theory is limited, mainly using engineering testing technology and computer numerical simulation technology. The research method of the theory is mainly limited to using engineering testing technology and numerical simulation technology. Liu et al. (2013) conducted an in-depth study on the key construction technology aspects of the TDM, such as earthwork excavation, joint nodes, permanent column pouring and postcasting belts, which were also introduced in detail. However, due to the different characteristics and objective conditions of the project, the key construction technologies should be constantly updated. Therefore, numerous engineering cases are needed to provide sufficient reference information.

In the study of soil characteristics, Yoo and Lee (2008) established a two-dimensional numerical model in which the model adopted hardened soil constitutive properties to study the characteristics of surface soil displacement. Wang et al. (2012) obtained the soil hardening model parameters of each soil layer through a series of consolidation tests of typical soil samples in Shanghai, which provided a reference for the subsequent study of soil hardening model parameters.

In terms of the deformation characteristics of structures designed using the TDM, Tan (2015) and Tan and Li (2011) studied subway foundation pit engineering with different excavation methods under four identical supporting systems. They found that the deformation of the enclosure structure can be effectively controlled by quickly pouring off the bottom plate after the excavation of the deep foundation pit in the soft soil area. Tan and Wang (2013a, 2013b) also analyzed the lateral wall displacement of foundation pit, diaphragm wall settlement, ground settlement, basement uplift, pore water pressure variation, etc. Meanwhile, they studied the deformation shape of a large foundation pit in the Shanghai soft soil layer, as well as the influence of foundation pit geometry and size on excavation deformation. Tang and Zhao (2016) studied the interaction mechanism between the soil and the structure in pile foundations and applied his theory to practical projects with the reverse method. The settlement, differential settlement and horizontal deformation of the supporting structure and pile, as well as the changes in soil pressure and retaining structure stress values in the foundation pit, were discussed during the construction based on TDM. The theory can effectively predict the actual changes in the project. Wang (2011) used MIDAS GTS to establish a finite element model of a foundation pit and simulated the entire excavation process, and they observed that the variations in the elastic modulus of the soil and internal friction angle values had a great influence on the deformation of the pile body of the foundation pit retaining structure. Wang (2012) conducted finite element analysis on specific engineering examples, and the relevant laws were summarized and compared with the actual monitoring data. The simulation results are available, but the impact of nearby buildings has not been considered during the construction process.

By summarizing the previous studies, it is found that different scholars always have unique opinions on both the key construction technology in the reverse method and the study of foundation pit deformation, but there are similar rules in different conclusions, and much work is still needed to make the reverse method technology more mature. Moreover, there is a lack of research on the key processes of reverse construction under complex environmental conditions. Hence, taking a super high-rise project as an example, this study analyzes the internal force and displacement characteristics of each structural component in TDM construction. The research model comprehensively considers soil that may be affected by excavation and the structural load of the surrounding buildings. Referring to the code, load combinations of the superstructure, including wind and earthquakes, are set up, and an elaborate simulation is carried out according to the actual construction sequence. The calculated settlement and stress results are compared with the measured values to verify the credibility of the model. This research provides reference value for subsequent construction and lays the foundation for the subsequent study of structural optimization.

2. Engineering project description

2.1. General situation of foundation pit

The object of this study is the second phase of Nanjing Jinmao International Square, which consists of three parts: tower, podium and basement. The tower is designed to have 68 floors and it is 308 m high, belonging to the super high-rise building class. It adopts a mixed structural system of frames and core tubes. The podium building is a cast-in-place reinforced concrete frame structure with 7 floors, and a height of 39.5 m (Figure 1).

Because the construction site is located in an urban center and the construction space is small, this project adopts top-down construction. The trapezoidal core tube area uses the underground diaphragm wall for support, and the other areas are supported by a large-diameter

a) **Project design renderings**   b) **Plan of the foundation pit**
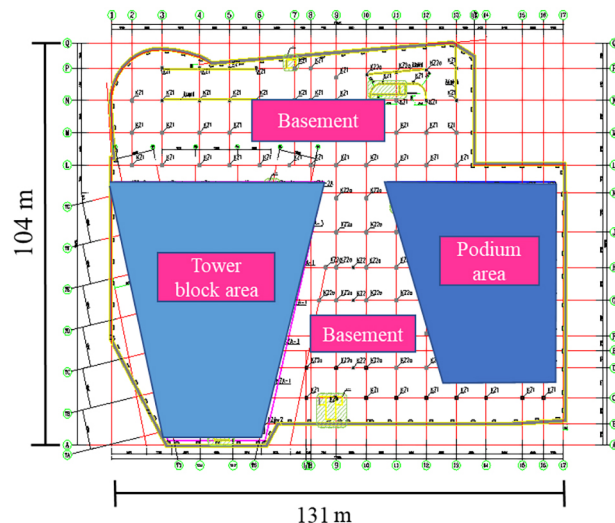

Figure 1. The foundation ditch and surrounding buildings

bored pile foundation under the columns, namely, "one column and one pile". The diameter of the pile foundation is 2.6 m, which is the largest at home and abroad and requires high construction technology.

To ensure the smooth progress of the full inversion method and reduce the intermittent period of construction, it is necessary to accelerate the underground construction progress and increase the number of upper support layers.

2.2. Model assumptions and material parameters

Due to the complexity of foundation pit engineering, this paper uses finite element analysis to establish the reverse construction process of underground structures. Reasonable assumptions and simplifications are as follows.

1) The soil is assumed to be elastic plastic, its stress and strain do not change with time, and the influence of construction torsion is not considered. The soil is considered to be continuous and uniform. In this study, the soil adopts the modified Mohr-Coulomb model (Wang, 2020) combining the nonlinear elastic and elastic properties of the material, and the solid elements are selected for simulation. The soil mass parameters are shown in Table 1.

2) In this model, for which the supporting structure system shown in Figure 2, is mainly composed of an underground diaphragm wall, one pile with one column and a bracing beam. The linear elastic constitutive relation is adopted, plastic changes are not considered, and the materials are homogeneous, continuous and isotropic.

3) Because the depth of the diaphragm wall is deep and measures for managing water and dewatering have been implemented before excavation, this simulation does not consider the influence of groundwater level and soil seepage, combined with the actual situation of this project.
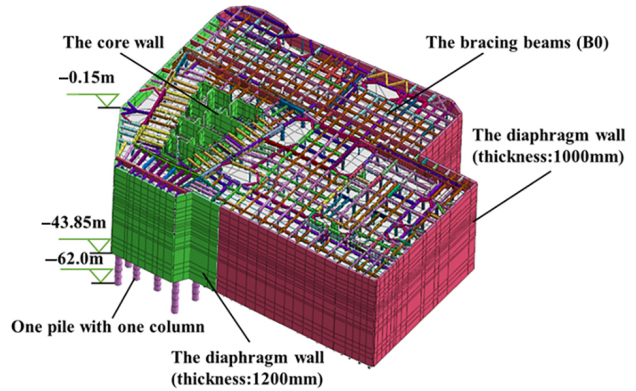

Figure 2. Diagram of the supporting structures

4) The floor and diaphragm wall are reinforced concrete structures that are set as plate elements. The beam structure and columns are all simulated by beam elements, and the piles adopt the implantable beam element. The dimensions and performance parameters of each structure in the engineering project of this paper are shown in Tables 2–5.

According to the detailed investigation report of geotechnical engineering (Jiangsu Nanjing Geo-Engineering Surveyiec Institute, 2014), the main physical indices and compression indices of the soil layer are shown in Table 1. Among the soil parameters, E_{50}^{ref} is the reference secant modulus, E_{oed}^{ref} is the reference tangent modulus, and E_{ur}^{ref} is the reference offloading and reloading modulus. Referring to the relational expressions of several elastic moduli given by Wang et al. (2019), the values of the modulus terms described above can be obtained based on the compression modulus $E_{S_{0.1-0.2}}$. The foundation plate of this project is located in the silty clay layer (③2), and the pile foundation bearing layer is the middle weathered tuff layer (⑤2).

Figure 2 shows the construction status of the support structures when the excavation is 8.5 m deep, taking the B0 layer as an example. Outsourced concrete columns

Table 1. Physical and mechanical properties of soil

Soil layer No	Soil description	γ (kN/m³)	C_{uu} (kPa)	φ_{uu} (°)	$E_{S_{0.1-0.2}}$ (MPa)	E_{50}^{ref} (MPa)	E_{oed}^{ref} (MPa)	E_{ur}^{ref} (MPa)
①	Fill clay	17.5	17	10.2				
②1	Silty clay mixed with silt and silt	19.6	9.1	17.4	8.19	9.58	7.37	46.68
②2	mucky clay	18.4	23.4	12.9	3.84	4.49	3.46	21.89
②3	Silty Clay	19.8	39.8	15.4	6.56	7.68	5.90	37.39
③1	Silty Clay	19.9	44.9	15.2	7.58	8.87	6.82	90.96
③2	Silty Clay	19.7	30.2	14.5	5.96	6.97	5.36	71.52
③3	Silty Clay	19.4	35.4	13.3	5.44	6.36	4.90	65.28
④	Silty clay mixed with gravel	20	50	22	9	10.53	8.10	108.00
⑤1	Strongly weathered-tuff	21	480	30	15	17.55	13.50	180.00
⑤2	middle weathered-tuff	24	6200	48.84				

Table 2. Column parameters

Number		1	2	3	4	5
Thickness (mm)		25	25	40	40	80
Column size (mm)	Pre-construction	525	575	1240	960	1600
	after construction	900	900	2000	1700	1600
Steel pipe diameter (mm)		525	575	1240	960	—
Poisson ratio		0.2	0.2	0.2	0.2	0.2
Equivalent elastic modulus (10^4 MPa)	Pre-construction	6.45	6.20	5.52	6.09	6.59
	after construction	4.25	4.57	4.07	4.11	6.59

Table 3. Pile foundation parameters

Name of the pile	Diameter (mm)	Length (m)	Strength grades	Design value of pile bearing capacity (kN)	Single-pile vertical endurance value features (kN)	Elastic Modulus (10^4 MPa)	Poisson ratio
ZH1	2600	27.5–34.55	C55	108000	85000	3.55	0.2
ZH2	2600	27	C45	89000	50000	3.35	0.2
ZH3	1800	22.55	C45	36000	23000	3.35	0.2
ZH4	1400	23	C45	22000	15000	3.35	0.2
ZH5	1200	20.55	C45	16200	11500	3.35	0.2
ZH6	1000	18–19	C55	13500	10900	3.55	0.2
ZH7	800	20	C45	7200	4500	3.35	0.2
ZH8	800	20	C55	7200	4500	3.55	0.2

Table 4. Typical beam parameters

Name of the beam	Element type	Section size (mm)	Equivalent elastic modulus (10^4 MPa)	Poisson ratio
BL101	beam	900×600	3.725	0.2
BL111	beam	900×1000	3.427	0.2
BL121	beam	1000×600	3.565	0.2
BL219	beam	1200×600	3.698	0.2
BL332	beam	1000×900	3.496	0.2

Table 5. Other structural component parameters

Structural component	Element type	Section thickness (mm)	Natural weight-specific density (kN/m³)	Equivalent elastic modulus (10^4 MPa)	Poisson ratio
Structural slab	plate	300	25	3.35	0.2
Raft foundation	plate	2800	25	3.45	0.2
Underground diaphragm wall	plate	1000, 1200	25	3.35	0.2
Wall of the core	plate	1000, 800	25	3.65	0.2

are commonly used in high-rise buildings, the combined stiffness of the external concrete-filled steel tube column adopts the conversion method commonly used in the specification and literature, and the converted stiffness is obtained by superimposed axial compression stiffness of steel tube and concrete (Cai, 2003). The stiffness conversion formula of the concrete-filled steel tube is:

$$E_{sc} = \frac{E_c A_c + E_s A_s}{A_c + A_s}, \tag{1}$$

where E_c and E_s are the axial compression stiffness values of the concrete and steel pipes respectively; A_c and A_s are the compression areas of concrete and steel pipes.

The key construction step of a pile-column is to lay down the steel cage after drilling the hole and insert the steel pipe in the upper part of the steel cage, and the depth of the steel cage is the position of the bottom plate. After the measurement and positioning, all of the concrete is poured. The former becomes the pile, and the latter becomes the vertical element of the common supporting structure of the column. After the reverse construction of the structure is completed, the steel pipe column can be outfitted with concrete to form a structural column, as shown in Figure 3. The steel pipe material of the columns is HRB400, and the material parameters of the columns are shown in Table 2.
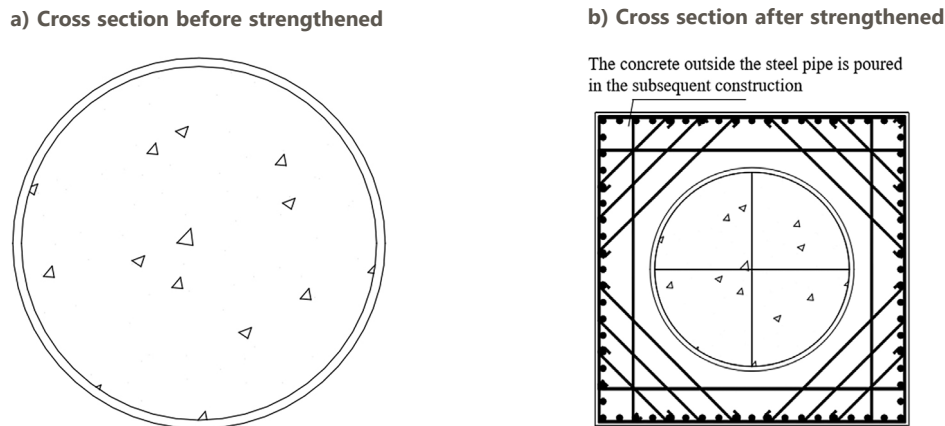
a) Cross section before strengthened

b) Cross section after strengthened

The concrete outside the steel pipe is poured in the subsequent construction

Figure 3. Column reinforcement diagram
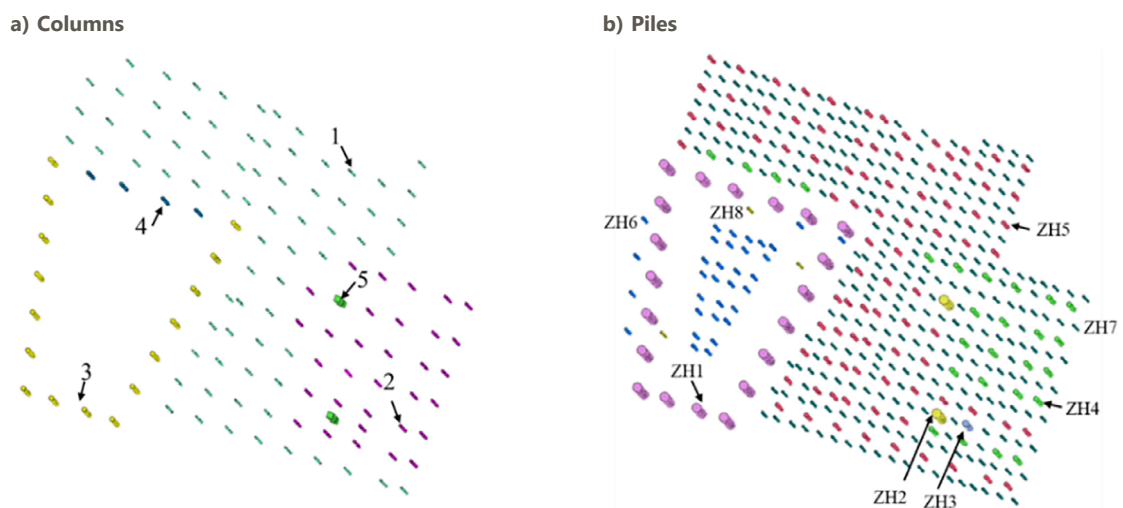
a) Columns

b) Piles

Figure 4. Placement of piles and columns

In addition, the arrangement of the columns and piles is shown in Figure 4, and the material parameters of the piles are shown in Table 3.
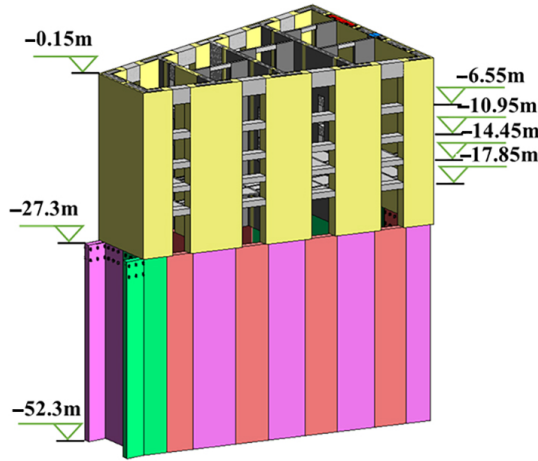
2.3. Design of the retaining structure

In this project, a foundation form shared by the diaphragm wall and the core tube structure are adopted for the first time. The wall of the core tube extends downward to bear the vertical load as the foundation of the core tube of the tower (Figure 5a). Because the thickness of the ground wall is independent of the thickness under the raft, the bearing capacity of the ground wall can be further improved, and the requirements on the shear capacity of the raft caused by the pile can be alleviated.

The tower column is in the form of a large-diameter pile (one column with one pile), which means that only one column and engineering pile are set at the position of the structural column, and a permanent concrete filled steel tube structural column is adopted. One column with one pile is widely used in reverse construction because of its advantages of simple structure, convenient construction and economical application.

According to the Technical Standard for the top-down method of building engineering, JGJ 432-2018, (Ministry of Housing and Urban-Rural Construction of the People's Republic of China, 2018), the equivalent model of the support column is fixed at one end and hinged at the other, as shown in Figure 6. When the foundation soil is hard soil or bedrock, the distance between the excavation face and the upper floor slab is selected for calculating the height. When the foundation soil is soft, the calculation length should be increased.

The beams and plates of each underground layer are horizontal supporting structures and the piles are vertical supporting structures. In the process of simplified calculation of pile force, the stiffness of the floor structure is assumed to be infinite and the horizontal displacement is approximately zero because of its large stiffness. When the floor pouring is completed, the upper end of the bottom pile is fixed in the floor and can be regarded as a rigid joint, and the bottom of the pile inserted into the soil is regarded as a rigid joint. The calculation model is shown in the Figure 7.

a) The core wall   **b) One column with one pile**
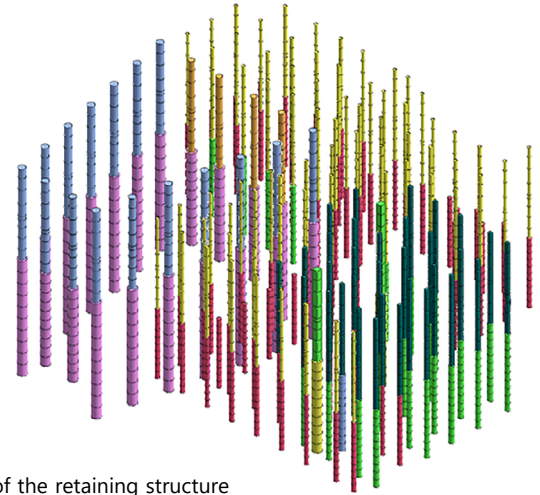

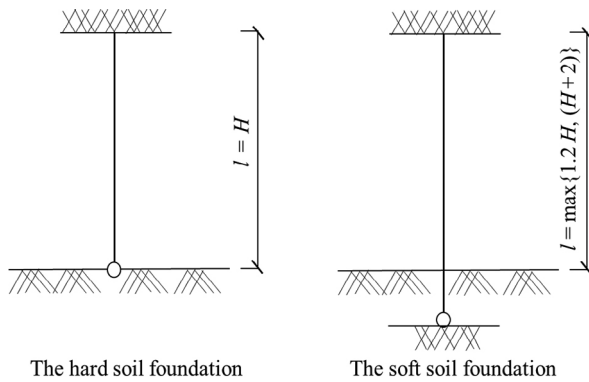**Figure 5.** Three-dimensional diagram of the retaining structure

Figure 6. The equivalent model of the support column

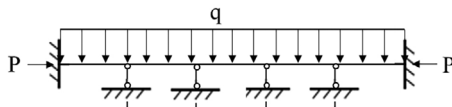**Figure 7.** Simplified model of pile under normal force

Figure 8. Simplified model of underground beam plates (Wang, 2020)

The underground floor structure can be regarded as a horizontal continuous beam with infinite rigidity. As shown in Figure 8, the connection between the side column and the beam plate is regarded as fixed support, the self-weight load of the superstructure and the construction load borne by the floor structure can be simplified as a uniform load (q), and both ends of the plate are subjected to horizontal soil pressure (P).

Based on the theory of the interaction between the superstructure and the foundation (Zhao, 1998), the general equation used in both the bottom-up method (BUM) and in TDM construction is:

$$\left(\left[K_b + K_r + K_{sp} \right] \right) \{U_b\} = \{S_b\} + \{P_r\}, \tag{2}$$

where K_b is the condensed equivalent stiffness matrix at the boundary between the superstructure and foundation, K_r is the equivalent stiffness matrix of the bottom slab, K_{sp} is the equivalent stiffness matrix of the soil–pile interaction system, $\{U_b\}$ is the boundary displacement vector, $\{S_b\}$ is
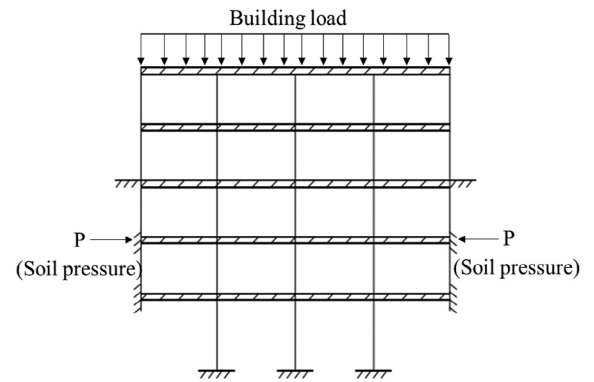
the boundary load vector condensed, and $\{P_r\}$ is the corresponding load vector.

In this paper, the interaction between a vertical bearing system composed of a diaphragm wall, piles and soil is considered. Based on Eqn (2), the theoretical analysis model is proposed as follows:

$$\left(\left[K_b + K_r + K_{spw} \right] \right) \{U_b\} = \{S_b\} + \{P_r\} + \{P_s\}, \tag{3}$$

where $\{P_s\}$ is the load on the soil range affected by the foundation pit, and K_{spw} is the corresponding equivalent stiffness matrix of the soil-pile-wall interaction system, which can be expressed as

$$K_{spw} = \begin{bmatrix} K_{ss} & K_{sp} & K_{sw} \\ K_{ps} & K_{pp} & K_{pw} \\ K_{ws} & K_{wp} & K_{ww} \end{bmatrix}. \tag{4}$$

The interface element in MIDAS can be used to estimate the interaction behavior of soil and structure. Some scholars found that the shear failure surface of the contact surface conforms to the Mohr-Coulomb shear failure criterion (Li et al., 2022). The cohesion force and friction angle of the Coulomb friction interface are R′(C_{soil}, j_{soil}), where R is the strength reduction coefficient of the structure and adjacent soil characteristics. The experience values of R are shown in Table 6.

Table 6. The experience values of strength reduction coefficient

| Sand/Steel	Clay/Steel	Sand/Concrete	Clay/Concrete
R = 0.6 ~ 0.7	R = 0.5	R = 1.0 ~ 0.8	R = 1.0 ~ 0.7

According to the settings that come with the software, soil–wall interaction is simulated with a 0.1 mm-thickness interface element. The interfacial strength reduction factor R is set as 0.7, considering the separation and slip characteristics of soil–wall interaction (Han et al., 2023).

3. Simulated analyses

3.1. Finite element model

In this study, combined with the nonlinear elastic and elastic–plastic properties of materials, a three-dimensional finite element model including the layered soil layer, supporting structure, layered excavation conditions and surrounding environment under actual working conditions is created, and a reasonable calculation domain and boundary conditions for the actual situation are established.

This paper relies on numerical calculation finite element software MIDAS/GTS to analyze the excavation and support process of deep foundation pit. Based on finite element analysis theory, MIDAS/GTS is implanted with the latest technology in geotechnical and tunnel engineering.
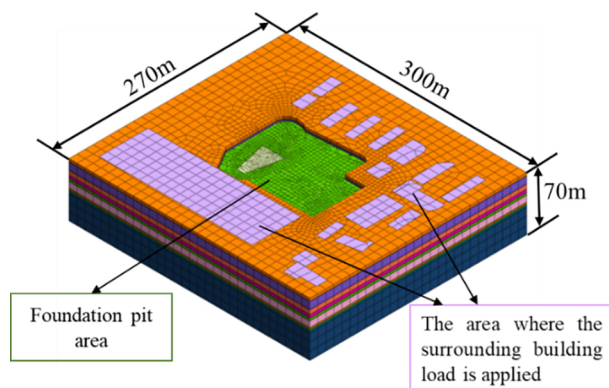

Figure 9. The calculation area of foundation

The successful application of GTS in many major projects at home and abroad has been widely recognized by geotechnical and tunnel researchers.

Since the stratum has infinite extension but the influence area of construction activities is limited, the analysis range of the foundation is determined by eliminating the boundary effect of the foundation pit to determine the limited calculation area range of the model. In this project, the depth of the foundation is approximately 27.3 m, the depth of the ground joint wall is approximately 51 m, and the maximum size of the outside of the foundation pit is 131.625 m×105.558 m. Considering the influence zone of the foundation pit fully, the soil range should be greater than 3 times the depth of the foundation pit (Ministry of Housing and Urban-Rural Construction of the People's Republic of China, 2013). Therefore, the size of the soil is planned to be selected as 300 m×270 m×70 m, as shown in Figure 9.

According to the detailed geotechnical investigation report of the Nanjing International Square Phase II project, the soil layer of the calculated area can be roughly divided into 10 layers, as shown in Figure 10. Because the groundwater has dropped below 1 m during construction, the impact of groundwater is not considered in the modeling.

Generally, the top of the soil model is a free surface, while the bottom is in moderately weathered tuff, and the displacement and rotation angle can be ignored. Therefore, the displacement in the X, Y, and Z directions should be limited in the bottom, the lateral boundary of the soil model should be limited in the horizontal direction, and the front and rear boundary of the soil should be restricted in the Y direction. In MIDAS/GTS, all grid groups can be automatically constrained (as shown in Figure 11). The weight of the soil layer affects the structure, so this should be considered. Because the diaphragm wall is deep and measures for preventing water have been implemented before excavation, the groundwater has dropped below 1 m during construction, and the influence of groundwater can be ignored in the modeling. In addition, the piles and columns are constrained at the bottom to restrict the displacement in the Z direction.
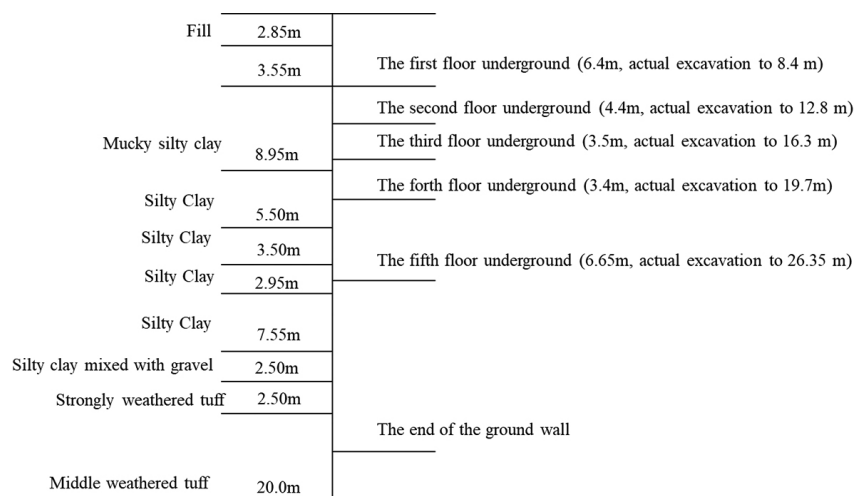
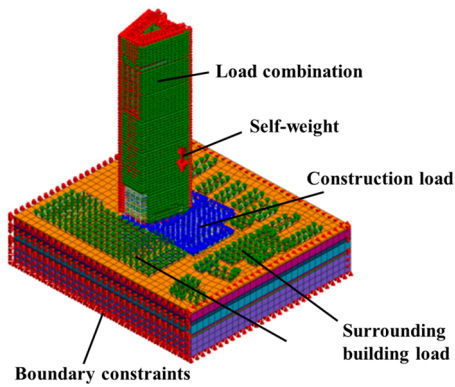
Figure 10. Soil layer distribution of foundation

Figure 11. Schematic diagram of the constraints and loads

According to the Technical specification for top-down construction method of underground building (JGJ 165-2010) (Ministry of Housing and Urban-Rural Construction of the People's Republic of China, 2010), for the combination controlled by the permanent load effect, the load component coefficient should be 1.35 and that of the variable load should be 1.4. With reference to the Technical specification for construction of top-down method (DG/TJ 08-2113-2021) (Ministry of Housing and Urban-Rural Construction of the People's Republic of China, 2021), we should consider the following loads and effects in the construction simulation calculations.

1) The value of the construction load on the floor of the construction platform should not be less than 10 kN/m². The construction load of the vehicle transport channel should not be less than 25 kN/m².

2) The rest of the floor construction live load should not be less than 1.5 kN/m².

3) When there are many upward floors, the structural strength should be checked under the wind load and seismic action. The basic wind pressure can be determined according to the 10-year recurrence period. We can calculate the earthquake load based on one earthquake every 10 years.

Therefore, the expression of load combination S is as follows:

$$S = 1.35S_{Gk} + 1.4S_{Qk} + 1.3S_{Ek} + 0.6S_{Wk}, \qquad (1)$$

where S_{Gk} is the permanent load, S_{Qk} is the variable load, S_{Wk} is the wind load and S_{Ek} is the seismic load. Table 7 shows the main loads according to the provisions of load combinations (Ministry of Housing and Urban-Rural Construction of the People's Republic of China, 2010).

3.2. Modeling analysis process

MIDAS/GTS is used to calculate and analyze the excavation and supporting process of the foundation pit with TDM, and the relevant data, such as soil settlement, ground diaphragm wall displacement, pile differential settlement, internal force of the supporting column, pile and ground diaphragm wall, are obtained under different working conditions. The calculation and analysis conditions are designed according to the actual construction of this project (Table 8).

Table 8. Calculation conditions

Calculation conditions	Number of underground excavation layers	Number of construction layers on the ground
1	1	10/19/38/49/68
2	2	10/15/25/35/38
3	3	10/15/25/35/38
4	4	10/15/25/35/38
5	5	10/15/25/35/38

Taking working Condition 1 as an example, the construction process is set as shown in Figure 12.

a) In the initial stress balance stage, activate the soil element with fixed boundary conditions and gravity. The load of the surrounding buildings is set as 10 kN/m² per floor;
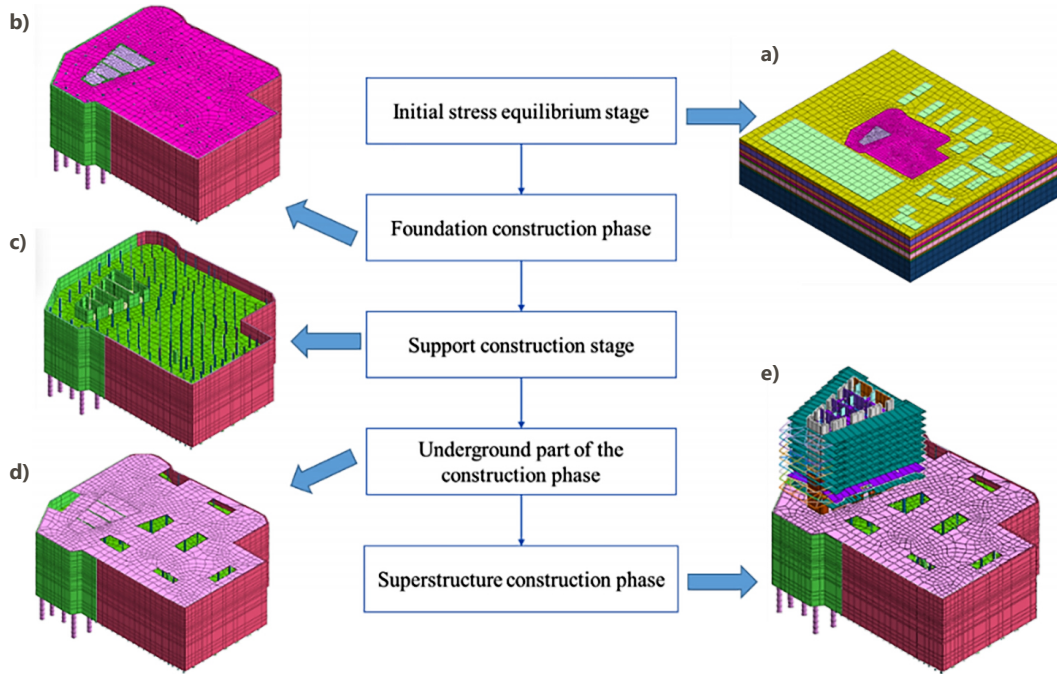
Table 7. Load combination

Load name	Location	Value
Building load	From 20F to WRF	Surface constant load and live load are adopted according to the structural construction drawings.
Construction load	19F	Live load is 10 kN/m²
	1F-18F	Live load is 1.5 kN/m²
The load of tower crane	1F	The z-direction envelope value of the steel foundation beam is taken from the calculation book "lifting Load of Boom Tower".
Position load of climbing formwork	1F	There are 38 machine positions, and 105 kN is applied at each site.
Constant load on beams	15F-WRF	The constant load of beams is calculated according to the density, thickness, and height of the partition wall.
Wind loads	1F-WRF	According to the national standard GB50009-2012 (Ministry of Housing and Urban-Rural Construction of the People's Republic of China, 2012), the basic wind pressure is 0.25kN/m² based on the 10-year recurrence period.
Earthquake loads	1F-WRF	The seismic load is taken value of the once-in-a-decade earthquake, based on the Code for Seismic Design of Buildings (GB50011-2016) (Ministry of Housing and Urban-Rural Construction of the People's Republic of China, 2016).

Figure 12. Numerical simulation process of the construction phase

b) In the foundation construction phase, activate the grid group of "one column and one pile" and the pile constraint;

c) In the support construction stage, activate the underground diaphragm wall, core shear wall, original column grid group and column constraints;

d) In the underground construction stage of working Condition 1, the actual excavation reaches 8.55 m, the soil grid of the first foundation pit is inactive, and the support grid group of the inner support beam and plate (located at –0.15 m) is activated;

e) In the construction phase of the superstructure, it is built up to 10, 19, 38, 49, 60 and 68 floors successively. The grid group of the core tube shear wall, beam, floor and column of the corresponding floors is activated, as well as the construction load and the load combination including wind, earthquake, structural live load and dead load.

3.3. Verification of analysis results

Taking working Condition 1 as an example, the displacement and internal force data of the main structural parts obtained from the simulation calculation are verified with the actual construction monitoring dates, and the arrangement of measuring points is shown in the Figure 13. The displacement measurement direction is vertical.

Combined with the layout of monitoring points for the core tube, the average values of settlement and internal force in the entire construction process (from floor 1 to floor 15) are collected in Tables 9–11. The detailed analysis is shown in Figure 14.

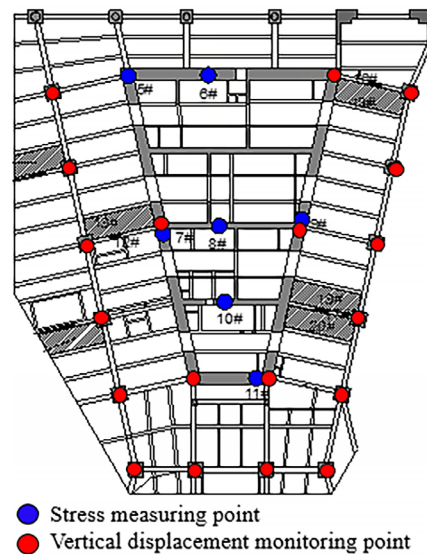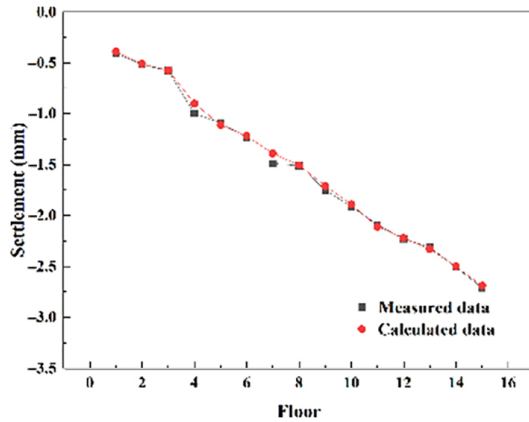The comparison between the numerical simulation analysis results and measured data in working Condition

1 (completion of B0 plate construction) shows that the deviations between calculation results such as settlement value and internal force value of continuous wall and measured data are mostly within 10%.

In addition, the pile settlement and axial force data in the entire construction process of working Condition 1 are collected. Figure 15 shows the comparison between the monitored values and calculation data, reflecting the change trend of vertical displacement and structural stress in the construction process.

Through the comparison, we found that the construction simulation analysis results are roughly consistent with the measured data, which verifies the correctness of the simulation analysis model.

● Stress measuring point
● Vertical displacement monitoring point

Figure 13. The measured responses' location

a) settlement

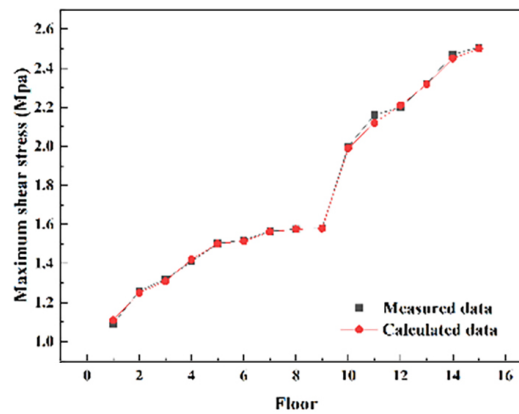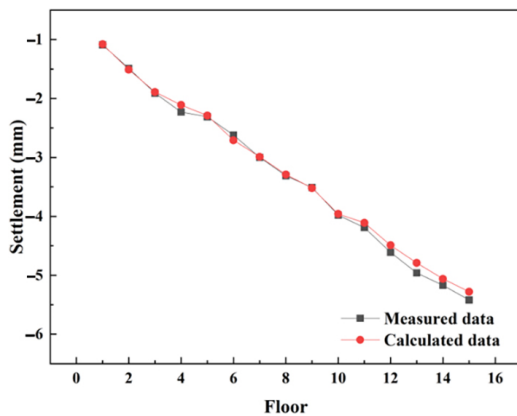b) maximum principal stress
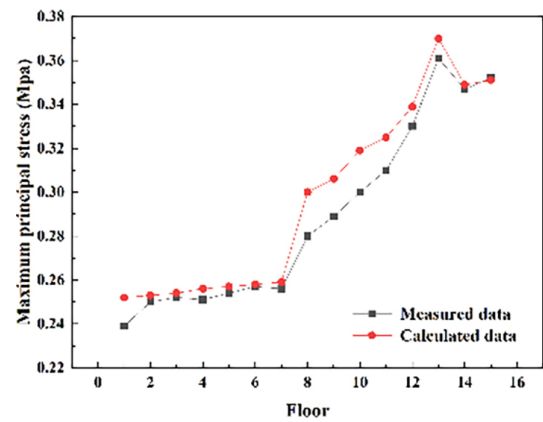
c) maximum shear stress

Figure 14. Comparison of calculated and measured data of the core tube
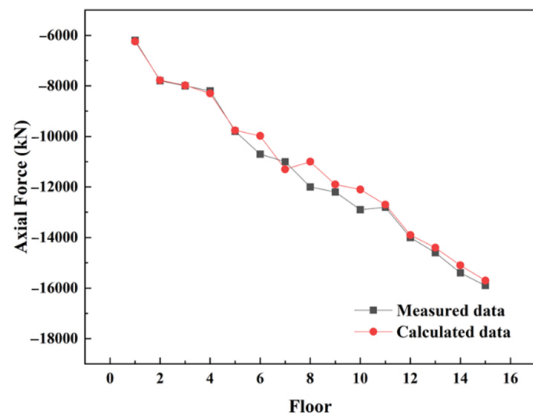
a) Settlement

b) Axial force

Figure 15. Comparison of calculated and measured data of "one column with one pile"

Table 9. Comparison of maximum settlement of the core tube

Floor	1	2	3	4	5	6	7	8	9	10	11	12	13	14	15
Measured data (mm)	0.41	0.52	0.58	1.00	1.09	1.23	1.49	1.51	1.75	1.91	2.09	2.23	2.31	2.51	2.71
Calculated data (mm)	0.39	0.51	0.57	0.90	1.11	1.22	1.39	1.51	1.71	1.89	2.11	2.22	2.33	2.50	2.69
Deviation (%)	−4.88	−1.54	−0.35	−9.92	1.84	−0.81	−6.71	0.27	−2.29	−1.05	0.96	−0.45	0.87	−0.32	−0.74

Table 10. Comparison of maximum principal stress of the core tube

Floor	1	2	3	4	5	6	7	8	9	10	11	12	13	14	15
Measured data (MPa)	0.239	0.250	0.252	0.251	0.254	0.257	0.256	0.280	0.289	0.3	0.310	0.330	0.360	0.347	0.352
Calculated data (MPa)	0.252	0.253	0.254	0.256	0.257	0.258	0.259	0.300	0.306	0.319	0.325	0.340	0.370	0.349	0.351
Deviation (%)	5.44	1.20	0.79	1.99	1.18	0.39	1.17	7.14	5.88	6.33	4.84	2.73	2.49	0.01	−0.28

Table 11. Comparison of maximum shear stress of the core tube

Floor	1	2	3	4	5	6	7	8	9	10	11	12	13	14	15
Measured data (MPa)	1.09	1.26	1.32	1.41	1.502	1.521	1.565	1.577	1.581	2	2.16	2.2	2.32	2.47	2.507
Calculated data (MPa)	1.11	1.25	1.31	1.42	1.501	1.514	1.562	1.575	1.58	1.99	2.12	2.21	2.317	2.45	2.5
Deviation (%)	1.84	−0.79	−0.76	0.71	−0.07	−0.46	−0.19	−0.13	−0.06	−0.50	−1.85	0.46	−0.13	−0.81	−0.28

Table 12. Excavation of working conditions

Information	Depth of excavation	Depth of horizontal support	The distance to the bottom	Underground floor construction
Case 1	−8.55	−0.15	−8.4	B0
Case 2	−12.95	−6.55	−6.4	B1
Case 3	−16.45	−10.95	−5.5	B2
Case 4	−19.85	−14.45	−5.4	B3
Case 5	−27.45	−24.5	−2.95	B4+Bottom slab

4. Results analysis and discussions

The excavation depth and floor data of underground construction under different working conditions are listed in Table 12. In this chapter, the calculation results of each working condition are sorted and compared according to the type of structural parts.

4.1. Maximum ground settlement

We summarize the settlement of the surrounding soil under various working conditions. Considering that the surrounding buildings have two basement layers, it should consider the vertical displacement change in the surrounding soil layer below −6.55 m should be considered.

Figure 16 reflects a similar change trend of soil settlement in all working conditions: the soil settlement of the surrounding soil increases obviously during excavation, while the settlement is almost unchanged during the construction of the superstructure. The deeper the excava-

tion is, the greater the soil settlement value. Moreover, the settlement differences between various conditions are positively correlated with the depth of horizontal support from the pit bottom.

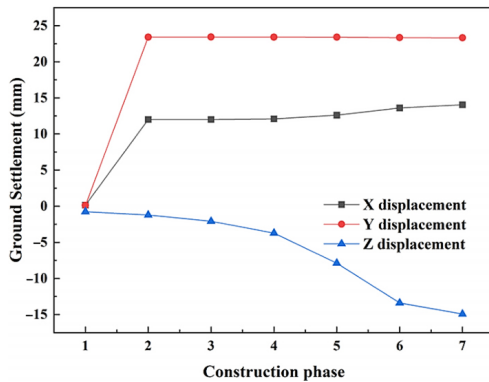### 4.2. Maximum displacement of the ground wall

Taking Working Conditions 1 and 5 as examples, we analyze the variation rule of diaphragm wall displacement with the progress of construction, as shown in the following tables and figures.

We can see in Figure 17 that during the process from Phase 1 to Phase 2, the displacement of the diaphragm walls increases in each condition. With the increase in the floors above, the X and Y displacements increase slowly, while the Z displacement slope is larger. The maximum Z displacement of the ground wall is mainly located in the core wall area.

The horizontal displacement values of the diaphragm walls in Condition 5 are greater than those in Condition 1. In the superstructure construction stage, the displacement differences are larger in Working Condition 1. Tables 12 and 13 show that when 38 floors are completed, the maximum value of settlement in Condition 1 increases from 0.75 mm to 7.88 mm, while the settlement in Condition 5 increases from 1.17 mm to 7.87 mm, and the increase in Condition 1 is larger. The X and Y displacements of working Condition 5 increase significantly during construction from Phase 4 to Phase 5 due to the large excavation depth. Therefore, we can see that the diaphragm wall's vertical displacement is determined by the superstructure's height, while its horizontal displacement is influenced by the excavation depth. The different excavation depths lead to different extrusions from the surrounding soil on the underground diaphragm wall.
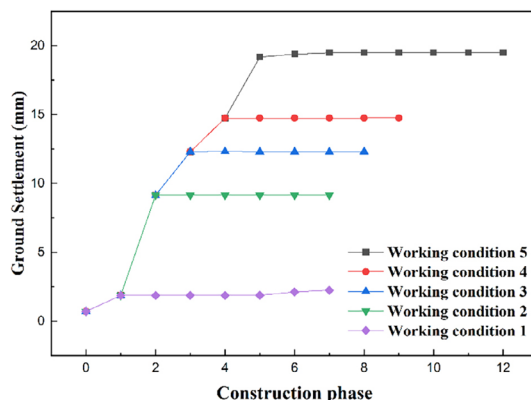
Figure 16. The maximum value of the surrounding soil settlement in each working condition

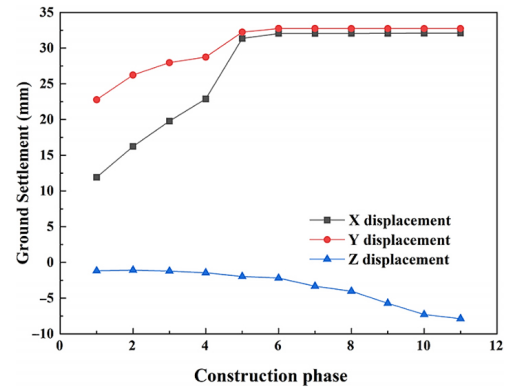a) Working Condition 1

b) Working Condition 5

Figure 17. Maximum displacement change of diaphragm wall with construction phase

Table 13. Change of the maximum displacement of ground wall in Working Condition 1

Construction content	Support construction	Dig down 1 layer	Build 10 floors	Build 19 floors	Build 38 floors	Build 60 floors	Build 68 floors
Phase	1	2	3	4	5	6	7
X displacement	0.15	12.01	12.01	12.1	12.6	13.6	14.05
Y displacement	0.11	23.42	23.43	23.42	23.4	23.34	23.32
Z displacement	−0.75	−1.21	−2.08	−3.72	−7.88	−13.39	−14.92

Considering that the Z-direction displacement changes significantly with the increase in the number of floors built above, the Z-direction displacements of the diaphragm wall under various working conditions are selected for comparison, as shown in Figure 18 and Table 14.

The trends of the working conditions are similar, and the displacement values increase with floor construction. Working Condition 2 shows the greatest increase in the Z-direction displacement of the ground diaphragm walls. The largest value of the Z-direction displacement occurs in Working Condition 5.

4.3. The maximum differential settlement between adjacent pile-columns

According to the variation in the differential settlement of the pile-columns in the construction stage, we compare the four working conditions from working Condition 2 to working Condition 5 (Figure 19).

From the variations in the maximum differential settlement of the pile-columns from working Condition 2 to working Condition 5 with the construction stage, it can be seen that the difference settlement in working Condition 5 is the smallest and that in working Condition 2 is the largest. Moreover, the maximum differential settlement values of the pile-column increase with the construction stage in all conditions.

To study the influence of superstructure construction layers on differential settlement, a comparative analysis of Working Conditions 1 and 5 is carried out. Figure 20 shows that the maximum differential settlement of the pile is pos-
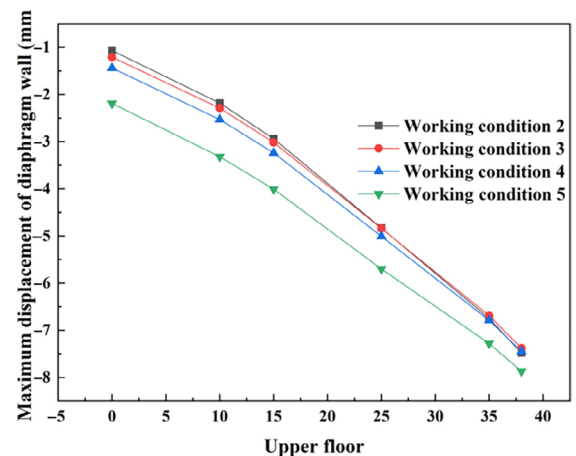

Figure 18. Variation in the maximum displacement of the diaphragm wall in each condition

itively correlated with the number of upper floors. With the increase in underground excavation layers, there are more supporting layers, and the differential settlement values between piles and columns are less. Due to the addition of the horizontal support structure, the overall stiffness is improved, increasing the structural stability. Therefore, the pile differential settlement value of working Condition 1 is the largest. Table 15 shows that when 38 floors are completed, the maximum value of settlement in Condition 1 is 20.63 mm exceeding the monitoring alert value 20 mm (Ministry of Housing and Urban-Rural Construction of the People's Republic of China, 2013), while the settlement in Condition 5 is 9.32 mm, which is in the safe range.

Table 14. Change of the maximum displacement of diaphragm wall in the Condition 5
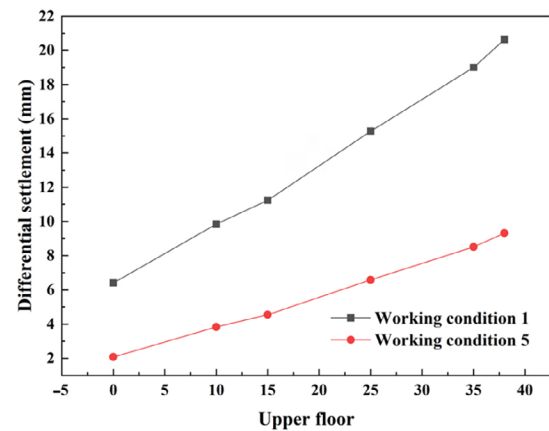
Construction content	Phase	X displacement	Y displacement	Z displacement
Dig down 1 layer	1	11.92	22.77	−1.17
Dig down 2 layers	2	16.24	26.23	−1.07
Dig down 3 layers	3	19.78	27.97	−1.21
Dig down 4 layers	4	22.88	28.75	−1.44
Dig down 5 layers	5	31.34	32.24	−1.96
Bottom construction	6	32.05	32.75	−2.19
Build 10 floors above	7	32.04	32.75	−3.32
Build 15 floors above	8	32.05	32.74	−4.01
Build 25 floors above	9	32.06	32.74	−5.7
Build 35 floors above	10	32.08	32.74	−7.28
Build 38 floors above	11	32.09	32.74	−7.87
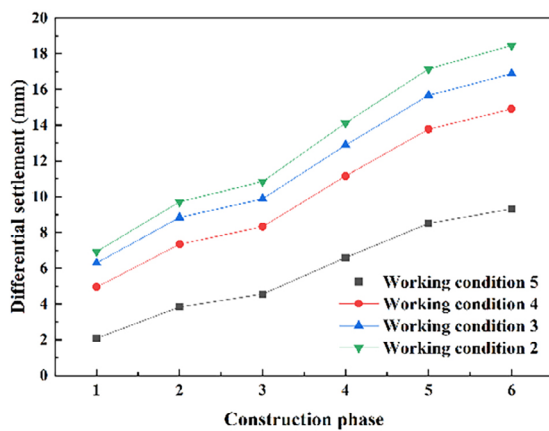
Figure 19. The maximum values of the differential settlement of the pile-columns

Figure 20. The differential settlement of piles-column varies with the floor

Table 15. The differential settlement of pile-column varies with the upper floor (mm)

Upper floor	0	10	15	25	35	38
Working condition 1	6.41	9.84	11.24	15.28	19.01	20.63
Working condition 5	2.08	3.83	4.55	6.59	8.51	9.32

4.4. Computed axial forces on the piles and columns

For the construction phase of the upper floors from Working Conditions 1 to 5, the calculated maximum axial force values of the columns and piles are listed in Table 16. Figure 21 shows that the variation trends of the maximum values of the column axial force in each working condition are mostly consistent with the floor construction. The value of working Condition 5 is the largest, and that of Condition 1 is the smallest. Similarly, the maximum value of the pile axial force in Condition 5 is the largest, and the minimum value occurs in Condition 2. Moreover, the maximum values of the pile axial force have the same change trends in each condition. For the supporting columns and piles, the more underground excavation layers there are, the greater the axial force.

4.5. Computed stress of the diaphragm wall

Taking Condition 5 as an exampl\e, we analyze the change rule of the internal force of the diaphragm wall with the construction stage, as shown in Figure 22. According to the trend chart of diaphragm wall stress in Working Condition 5, we can see that the stress rises greatly during underground construction and remains unchanged when the superstructure construction begins. Figure 23 shows the stress distribution of the diaphragm wall in construction phase 11. The maximum principal stress value is 13 MPa, and the maximum shear stress value is 6.5 MPa, both of which meet the strength requirements of the structure.
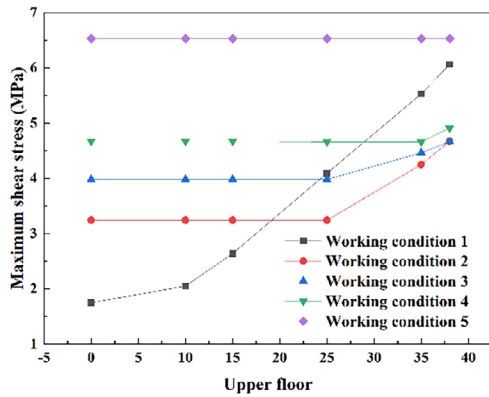
Comparisons of the maximum shear stress of the superstructure for each condition are shown in Figure 24. The shear stress in Working Condition 5 is the largest and remains unchanged. In Working Condition 1, the shear force is minimal after underground construction and then enriched with the upper floor, with the largest increase. In addition, the maximum principal stress values of the diaphragm wall in each condition do not change with the increase in the upper floor. The excavation depth of the condition is larger, and the maximum principal stress value is larger. The stress value gap of each working condition is positively correlated with the depth between the support system and the pit bottom after underground excavation.

Table 16. The maximum internal force of columns and piles (unit: 10^6N)

Upper floor	Structure	0	10	15	25	35	38
Working Condition 1	columns	−2.21	−12.47	−15.23	−23	−29.9	−32.87
	piles	−12.1	−14.64	−16.02	−20.56	−24.8	−26.68
Working Condition 2	columns	−3.59	−13.15	−15.88	−23.53	−30.23	−33.2
	piles	−9.37	−10.48	−11	−13.63	−19.5	−22.38
Working Condition 3	columns	−4.88	−14.26	−16.94	−24.46	−31.12	−34.29
	piles	−8.52	−9.69	−10.24	−14.21	−21.17	−24.08
Working Condition 4	columns	−6.53	−15.12	−17.8	−25.3	−31.96	−35.33
	piles	−8.25	−10.07	−11.42	−16.7	−24.48	−27.85
Working Condition 5	columns	−8.52	−16.5	−19.29	−27.14	−34.23	−37.7
	piles	−34.02	−41.78	−43.01	−46.92	−50.59	−52.18

a) The maximum axial force of columns
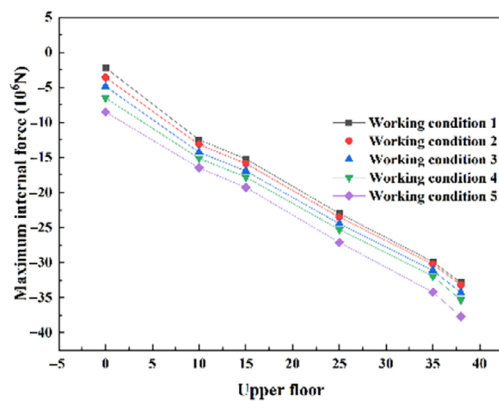
b) The maximum axial force of piles
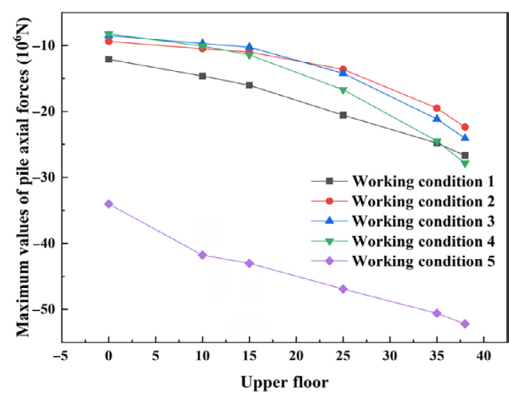
Figure 21. The maximum axial force of columns and piles change in each working condition
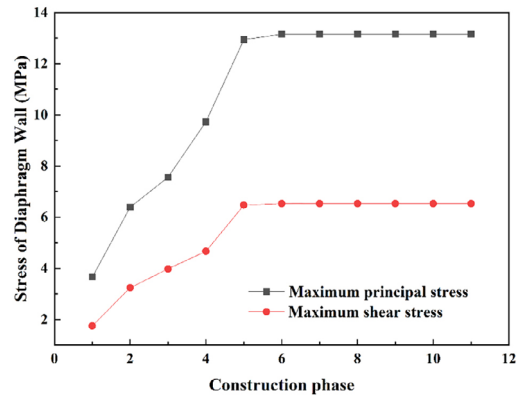
Figure 22. Variation of the diaphragm wall stress in Condition 5 with the construction stage

a) Maximum principal stress
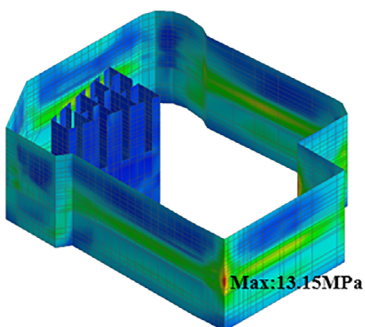
b) Maximum shear stress
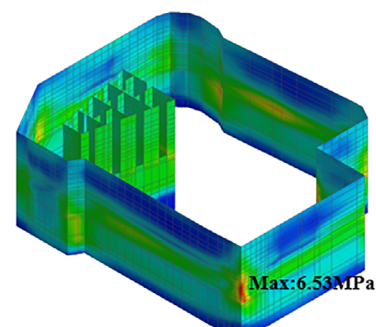
Figure 23. Variation of the diaphragm wall stress in Condition 5 with the construction stage

a) Maximum shear stress
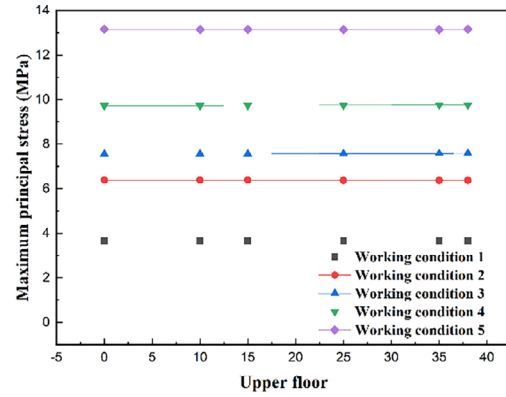
b) Maximum principal stress

Figure 24. Comparison of maximum stress of the diaphragm wall in each Working Condition
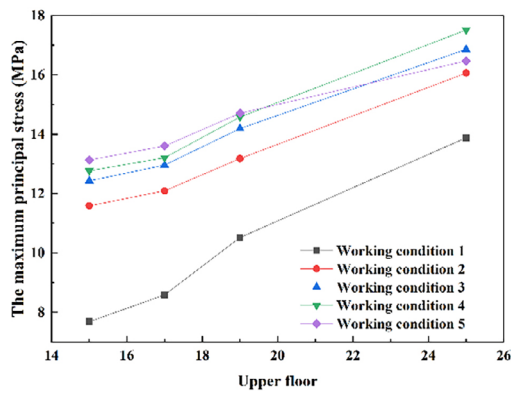

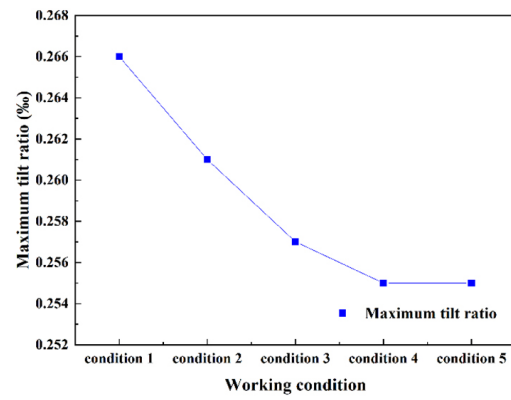Figure 25. Comparison of the maximum principal stress of the supporting beam

Figure 26. Comparison of the maximum tilt rate of the superstructure in each condition

4.6. Computed stress of the supporting beams

The maximum principal stress values of the underground supporting beam under different conditions are compared.

Figure 25 shows that the maximum principal stress value in Working Condition 1 is the smallest, while those of Working Conditions 2, 3, and 4 have the same variation trends. Because Working Condition 5 has built the bottom slab and there are more underground supporting layers, the slope of the maximum principal stress decreases with the number of floors. Therefore, the maximum principal stress value in Working Condition 5 after 20 floors is less than those of Working Conditions 3 and 4.

4.7. The inclination of the superstructure

Combined with the displacement of the superstructure in the X direction of each working condition, the maximum inclination ratio of the superstructure under each working condition is calculated, as shown in Table 17.

Table 17. The inclination of the superstructure

Working condition	Condition 1	Condition 2	Condition 3	Condition 4	Condition 5
Maximum incline (‰)	0.266	0.261	0.257	0.255	0.255

From the Table 17 and Figure 26, the maximum inclination ratio of the superstructure decreases with more underground supporting layers, improving the overall stiffness and structural stability. In addition, the maximum inclination ratio under each working condition is less than the standard limit of 2‰ (Ministry of Housing and Urban-Rural Construction of the People's Republic of China, 2011), which meets the safety requirements.

5. Conclusions

This research establishes a three-dimensional analysis model, including stratification of the soil layer, supporting structure, excavation condition, and surrounding buildings. The complete process of excavation is simulated by adopting a reasonable calculation domain and boundary conditions suitable for the actual situation. We summarize the main conclusions:

1. The changing trend of the surrounding soil settlement is similar in all working conditions. The settlement of surrounding soil increases obviously during excavation. The settlement remains almost unchanged in the construction of the superstructure. There is a positive correlation trend between the settlement difference and the corresponding horizontal support distance to the bottom in each working condition.

2. The maximum displacement value of the diaphragm wall is less than the alarm value. Changes in vertical displacement mainly depend on the height of the upper building. The horizontal displacement and the internal force of the diaphragm wall vary based on the depth of the excavation and the number of construction layers. Because the excavation leads to extrusion from the surrounding soil on the diaphragm wall.

3. The settlement differences of adjacent pile-columns rise with the superstructure floors. After excavation, more supporting layers reduce the differential settlement values between piles because the horizontal support structure is increased, improving the overall stiffness and enhancing the structural stability.

4. For the one column with one situation, the more underground excavation layers there are, the greater the axial force. The pile-columns on both sides of the core tube are subjected to a large axial force, which is positively correlated with the upper construction height. The axial forces during construction are less than the limit value of the vertical limit bearing capacity.

5. The stress values at the connections between the support beams and the diaphragm wall are large, and it is easy to see that they appear to be a weak link. The stress of the support beam should not exceed 80% of the design strength. The addition of the bottom slab improves the overall stiffness of the structure. Therefore, it is not appropriate to build too many layers prior to the bottom slab being completely constructed.

6. From the perspective of the bearing capacity, it is safe to choose the B0 layer for the interface layer. Summarizing the structural deformation characteristics during construction is a convenient way to prepare the subsequent estimation of the critical height and conduct the optimization of the related structure.

Data availability

Some or all data, models, or codes that support the findings of this study are available from the corresponding author upon reasonable request.

References

Cai, S.-H. (2003). *Modern steel tube confined concrete structure*. China Communications Press.

Han, J., Wang, J., Jia, D., Yan, F., Zhao, Y., Bai, X., Yan, N., Yang, G., & Liu, D. (2023). Construction technologies and mechanical effects of the pipe-jacking crossing anchor-cable group in soft stratum. *Frontiers in Earth Science*, *10*. https://doi.org/10.3389/feart.2022.1019801

Jiangsu Nanjing Geo-Engineering Surveyiec Institute. (2014). *The detailed investigation report of geotechnical engineering of Nanjing International Square Phase II* (Report No. 2014-GK001). Nanjing International Group Co., LTD (in Chinese).

Li, T., Zhao, W., Liu, R., Han, J., Jia, P., & Chen, C. (2022). Visualized direct shear test of the interface between gravelly sand and concrete pipe. *Canadian Geotechnical Journal*. https://doi.org/10.1139/cgj-2022-0007

Liu, Y., Li, J.-P., & Chen, W. (2013). Key construction techniques for oversized excavation pits using top-down method. *Chinese Journal of Geotechnical Engineering*, *35*(1), 489–494 (in Chinese).

Ministry of Housing and Urban-Rural Construction of the People's Republic of China. (2010). *Technical specification for top-down construction method of underground buildings* (JGJ165-2010). China Architecture and Building Press (in Chinese).

Ministry of Housing and Urban-Rural Construction of the People's Republic of China. (2011). *Code for design of building foundation* (GB50007-2011). China Architecture and Building Press (in Chinese).

Ministry of Housing and Urban-Rural Construction of the People's Republic of China. (2012). *Load code for the design of building structures* (GB50009-2012). China Architecture and Building Press (in Chinese).

Ministry of Housing and Urban-Rural Construction of the People's Republic of China. (2013). *Technical specifications for urban rail transit engineering monitoring* (GB50911-2013). China Architecture and Building Press (in Chinese).

Ministry of Housing and Urban-Rural Construction of the People's Republic of China. (2016). *Code for seismic design of buildings* (GB50011-2016). China Architecture and Building Press (in Chinese).

Ministry of Housing and Urban-Rural Construction of the People's Republic of China. (2018). *Technical standard for top-down method of building engineering* (JGJ 432-2018). China Architecture & Building Press (in Chinese).

Ministry of Housing and Urban-Rural Construction of the People's Republic of China. (2021). *Technical specification for construction of top-down method* (DG/TJ 08-2113-2021). China Architecture and Building Press (in Chinese).

Tan, Y. (2015). Lessons learned from construction of Shanghai metro stations: importance of quick excavation, prompt propping, timely casting and segmented construction. *Journal of Performance of Constructed Facilities*, *29*(4), Article 04014096. https://doi.org/10.1061/(ASCE)CF.1943-5509.0000599

Tan, Y., & Li, M. (2011). Measured performance of a 26m deep top-down excavation in downtown Shanghai. *Canadian Geotechnical Journal*, *48*(5), 704–719. https://doi.org/10.1139/t10-100

Tan, Y., & Wang, D. (2013a). Characteristics of a large-scale deep foundation pit excavated by the central-island technique in Shanghai soft clay. I: Bottom-up construction of the central cylindrical shaft. *Journal of Geotechnical and Geoenvironmental Engineering*, *139*(11), 1875–1893. https://doi.org/10.1061/(ASCE)GT.1943-5606.0000929

Tan, Y., & Wang, D. (2013b). Characteristics of a large-scale deep foundation pit excavated by the central-island technique in Shanghai soft clay. II: Bottom-up construction of the central cylindrical shaft. *Journal of Geotechnical and Geoenvironmental Engineering*, *139*(11), 1894–1910. https://doi.org/10.1061/(ASCE)GT.1943-5606.0000928

Tang, Y., & Zhao, X. (2016). Field testing and analysis during top-down construction of super-tall building in Shanghai. *KSCE Journal of Civil Engineering*, *20*(2), 647–661. https://doi.org/10.1007/s12205-015-1529-z

Wang, Y. G. (2011). *Design and case studies for top-down method construction*. China Architectural and Building Press (in Chinese).

Wang, Q.-L. (2012). *Top-down method technology in high-rise building in the applied research* [Doctoral dissertation]. Liaoning Technical University.

Wang, W.-H. (2020). *Study on pile-column conversion mechanism of top-down method in super high-rise buildings* [Doctoral dissertation]. Southeast University.

Wang, W.-d., Wang, H.-R., & Xu, Z.-H. (2012). Experimental study of parameters of hardening soil model for numerical analysis of excavations of foundation pits. *Rock and Soil Mechanics*, *33*(8), 2283–2290 (in Chinese). https://doi.org/10.3969/j.issn.1000-7598.2012.08.008

Wang, C., Huang, M., Ma, C.-R. (2019). Sensitivity analysis of stratum parameters to soft soil deep foundation pit deformation. *Bulletin of Science and Technology*, *35*(10), 171–175 (in Chinese). https://doi.org/10.13774/j.cnki.kjtb.2019.10.033

Yoo, C., & Lee, D. (2008). Deep excavation-induced ground surface movement characteristics – A numerical investigation. *Computers and Geotechnics*, *35*(2), 231–252. https://doi.org/10.1016/j.compgeo.2007.05.002

Zhao, X. H. (1998). *Theory of design of piled raft & piled box foundations for tall buildings in Shanghai*. Tongji University Press (in Chinese).